JOURNAL OF MATERIALS SCIENCE 28 (1993) 2061–2066

Evolution of grain shape and size during high-temperature creep of a yttria-doped fine-grained alumina

P. GRUFFEL, F. RIGHETTI*, C. CARRY
*Laboratoire de Céramique and *Département de Mathématique, Swiss Federal Institute of Technology, CH-1015 Lausanne, Switzerland*

A semi-automatic method of image analysis was used to characterize the evolution of the microstructure of a polycrystalline alumina in terms of grain size and grain shape during different thermomechanical treatments. This study showed that for this material normal grain growth occurs during compressive creep and annealing; in addition, during creep under certain conditions grains flatten in the direction of the applied stress. Three-dimensional estimation of the grain shape was performed by analysing differently oriented plane sections of the specimens.

1. Introduction

The study and characterization of microstructure are necessary in order to understand the relationships between the microstructure and properties of materials, and are two of the most important aspects of materials science. Generally, to study some features of a microstructure, two-dimensional polished and etched plane sections are examined with an optical or an electron microscope and the corresponding photographs are taken. The analysis of these photographs is often the only way to extract the desired information about the microstructure. A partial microstructural characterization can be easily obtained by manual measurements (for example, the mean grain size), but the use of computerized methods becomes unavoidable for a deeper statistical analysis such as the study of the distributions of the different parameters and their possible relationships. In the case of monophased polycrystalline materials, grain boundaries are thermally or chemically etched in such a way that every single grain of the polycrystal can be identified, allowing its characteristic parameters to be determined. A representation of the two-dimensional grain structure of a polycrystal can be considered as a two-dimensional cell-complex [1].

During high-temperature thermomechanical treatments of polycrystalline materials, it is well known that grains can grow and that their shape can change. The importance of these two phenomena depends on the material considered, the experimental conditions and the mechanism(s) producing the deformation. Grain growth during high-temperature deformation has been observed during superplastic creep on metallic [2, 3] and ceramic [4–7] materials. Grain shape modification is generally observed for dislocation and diffusional creep [8], but not during superplastic creep [9].

In this work a semi-automatic image analysis method was used to study the microstructural evolution during compressive creep of a fine-grained dense alumina; more details concerning this method are given in [1]. The microstructural evolution is characterized here in terms of the grain size and grain shape. The alumina studied had been doped with 500 p.p.m. MgO and 500 p.p.m. Y_2O_3 (by weight) in order to obtain a dense material with a fine grain size. The powder was hot-pressed at 1450 °C under vacuum in graphite dies. The creep behaviour of this material showed a range of grain size between 1.3 and 2.3 μm for which the strain rate is approximately constant in spite of grain growth and this range has been called the strain rate plateau [10, 11]. We were therefore especially interested in studying the evolution of the grain size distribution and that of the shape during this particular creep regime. For these different samples, analysis of plane sections oriented differently relative to the external stress were performed so that the three-dimensional shape of the grains and its evolution during the different thermomechanical treatments could be evaluated. The results are presented in the form of mean values, cumulative distributions and histograms. The normalized (divided by the mean value) grain size distributions are compared with the theoretical distributions. Grain shape changes are compared with the overall sample deformation here, but the mechanisms of deformation of this alumina, as well as grain growth, are discussed elsewhere [11].

2. Experimental procedure

We have already described hot-pressing and compressive creep test procedures in [10]. Microstructures were studied on polished and thermally etched plane

0022–2461

TABLE I Designations and thermomechanical treatments for the different samples

Code	Thermomechanical treatment
INI	Hot-pressed at 1450 °C for 15 min under 45 MPa under vacuum
AN	INI + annealing in air at 1450 °C for 654 min
DEF1	INI + deformation at 1450 °C under 20 MPa to $\varepsilon \approx -0.3$ in 213 min
DEF2	INI + deformation at 1450 °C under 20 MPa to $\varepsilon \approx -0.5$ in 500 min

sections in the centre of the specimen, and the etching temperature was held below the deformation temperature to avoid significant grain growth during this operation. The characteristics of the more significant samples, their designations and the conditions of their thermomechanical treatments are given in Table I; other deformed and annealed samples have been studied, but to avoid confusion they are not mentioned here. Characterized sections were chosen in well-defined orientations relative to the hot-pressing stress (P) and the deformation stress (σ) as shown in Fig. 1. Sections parallel to P (referred to as PAR) were characterized for all samples; moreover, in the deformed samples, these sections were also chosen parallel to σ. For the hot-pressed and annealed samples the section PER was normal to P, and for the deformed samples normal to σ. For each sample statistical analysis was performed on at least 1000 grains observed in five different fields.

The parameters of the microstructure which were used in this work were briefly as follows.

The mean grain size ($\bar{d}$), given by $1.38\bar{s}^{1/2}$, where $\bar{s}$ is the mean intercept area of the grain in a planar section [12]. This parameter is defined as a three-dimensional diameter.

The equivalent diameter (d), the diameter of the circle having the same area as the section of the grain considered.

The eccentricity (ecc), the eccentricity of the inertia ellipse associated with the grain considered. It is defined by $[1 - (b^2/a^2)]^{1/2}$ where a and b are, respectively, the major and minor axes of the inertia ellipse.

The direction, given by the angle between the major axis of the inertia ellipse and the horizontal axis Ox of the figure. Samples were carefully placed in the microscope and this axis was therefore perpendicular to the direction of P and parallel to σ in PAR sections.

The grain aspect ratio (GAR), given by $\bar{l}_{\parallel P}/\bar{l}_{\perp P}$, where $\bar{l}$ is the mean intercept length measured manually in a given direction; in this work $\bar{l}$ was measured parallel and perpendicular to P.

The feret diameter (fer_x), the length of the projection of the grain on the x-axis; fer_y is defined in a corresponding way.

The mean value of a parameter i is written $\langle i \rangle$ and is given by $\sum_j i_j/n$, where n is the number of grains.

3. Results and discussion

For the sake of illustration, one typical microstructure of the studied alumina is shown in Fig. 2 (sample INI

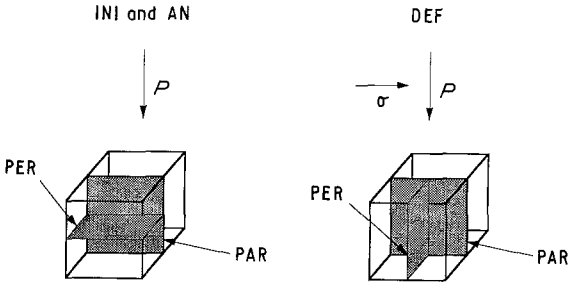

Figure 1 Orientation of the different sections studied relative to the referential given by the directions of P and σ.

of Table I); the corresponding binary image and the associated inertia ellipses are also shown in this figure. The binary image can be considered as a two-dimensional cell-complex and is used to perform quantitative analysis. In this image the limits of the grains are defined by points distributed along the grain boundaries, the number of points depending on the parameters that are chosen for one step of the image analysis procedure [1]. Fig. 3 shows the evolution of the strain rate ($\dot{\varepsilon}$) with time (t) under creep conditions for a uniaxial compressive stress of 20 MPa at 1450 °C; the strain rate plateau appeared clearly after 150 min. The strain level (ε) reached after 500 min under these conditions was -0.5. (The test was stopped at this strain level to maintain a uniaxial stress state in the middle part of the sample.) The evolution of $\bar{d}$ measured on the PAR section of the deformed samples is also shown in Fig. 3 and can be represented by a classical grain growth law given by

$$\bar{d}^3 - \bar{d}_0^3 = (3.7 \times 10^{-4})t \quad \mu m^3 s^{-1}$$

where $\bar{d}_0$ is the mean grain size after hot-pressing (referred to as the INI state in Table I). The exponent 3 is generally considered as a characteristic of the grain boundary migration-controlled solute drag of impurities or solute.

The mean parameters used in this work to characterize the grain shape were GAR and ecc. Their variation during creep is shown in Fig. 4. These parameters are nearly constant when the creep time is < 150 min (the period corresponding to a strain level of -0.25 under these conditions) and increase rapidly during the strain rate plateau. For the stress-free annealed samples these shape parameters did not show any significant difference from those for the hot-pressed samples.

In all cases $\langle ecc \rangle$ is greater than zero, the value that corresponds, from the definition of the eccentricity, to

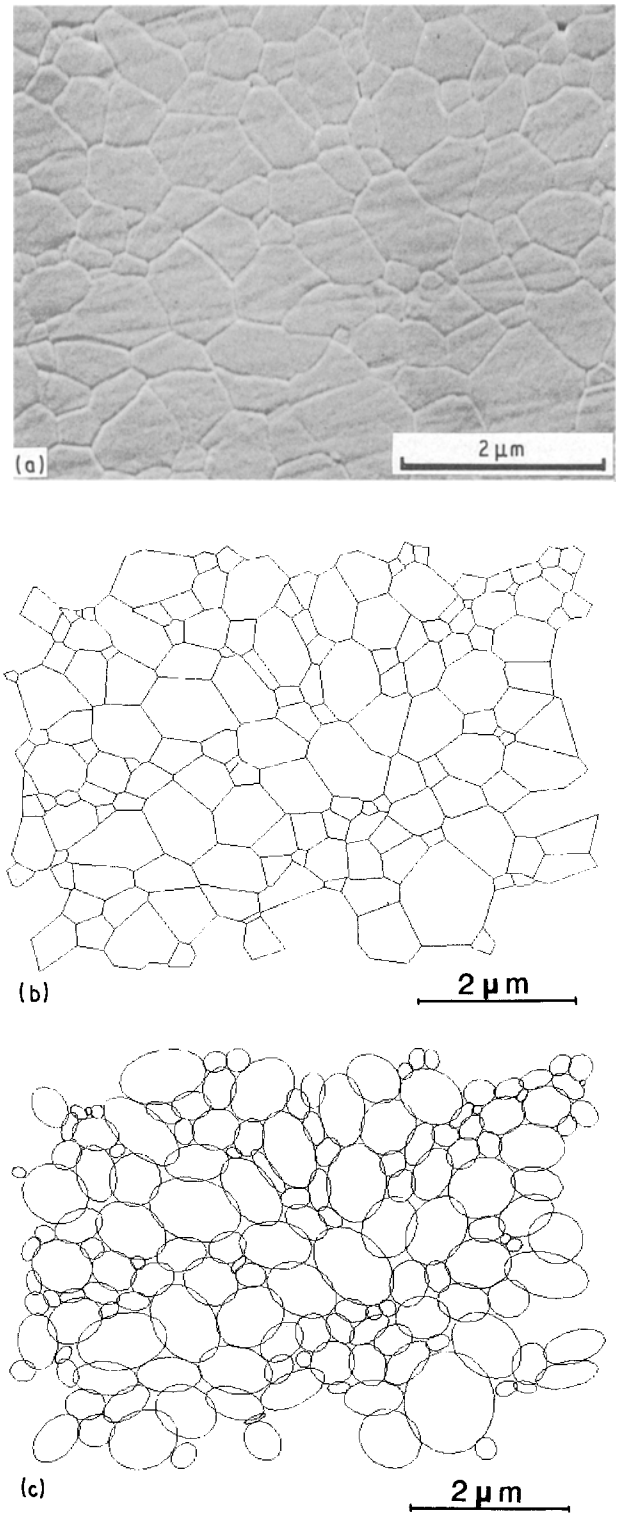

Figure 2 (a) Scanning electron micrograph of a typical microstructure of a dense polycrystalline alumina. (b) Corresponding two-dimensional cell complex and (c) inertia ellipses. Sample INI in Table I, $\bar{d} = 0.6$ μm.

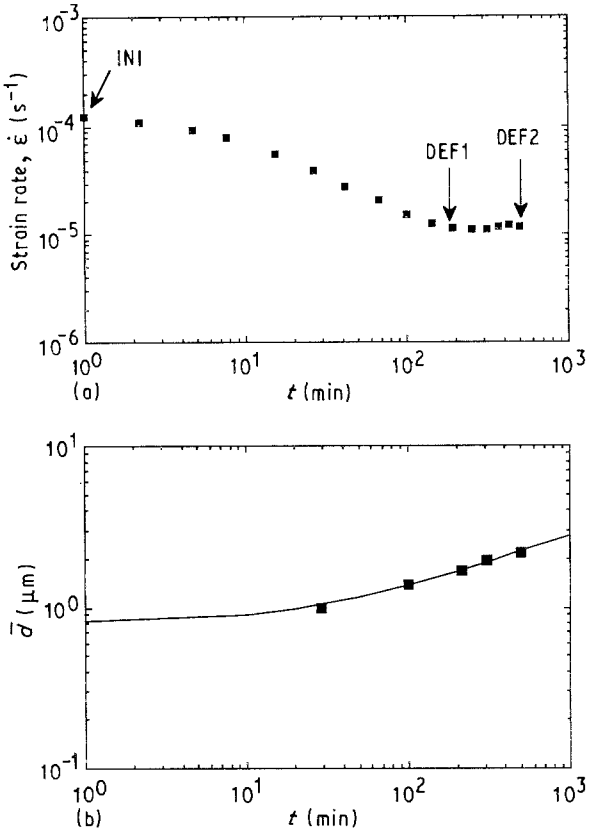

Figure 3 Evolution of (a) the strain rate ($\dot{\varepsilon}$) and (b) the mean grain size ($\bar{d}$) during creep in compression at 1450 °C under 20 MPa.

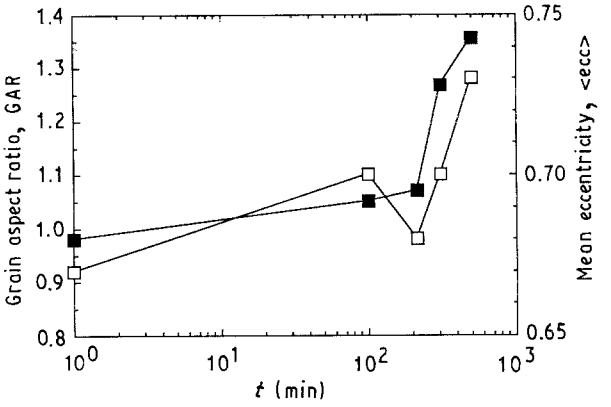

Figure 4 Evolution of the mean values of parameters used to characterize grain shape during creep in compression at 1450 °C under 20 MPa: (■) GAR and (□) ⟨ecc⟩.

a microstructure for which all grains are equiaxed. This result is also true for the samples having a GAR approximately equal to unity (see Fig. 4). Such a difference is due to the definition of these two parameters. On the one hand, ecc is related only to the shape of the grains, not to any external referential; on the other hand, GAR is related to the referential given here by the directions of P and σ. Consequently, a preferential orientation of the grains affects GAR but not ecc; as an example, a set of two-dimensional needles randomly orientated will have GAR=1 and ecc ≈ 1. The distribution functions of the grain orientations measured on the PAR section of different samples are shown in Fig. 5. In the hot-pressed state (INI) grains are slightly oriented in the direction perpendicular to P. After a deformation of -0.3, which correspond to the beginning of the plateau (DEF1), grains do not show a preferential orientation. If the deformation is extended to a strain level of -0.5 with half of the overall deformation occurring during the plateau (DEF2), the grains become oriented perpendicularly to σ. As in this PAR section P and σ are perpendicular, it can be concluded that the preferential orientation of the grains changes with deformation if the

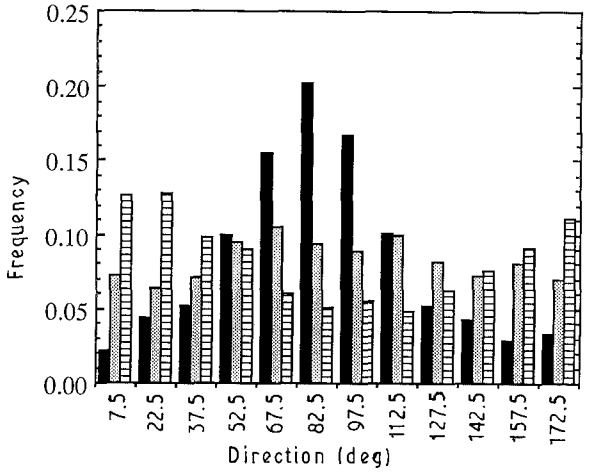

Figure 5 Distribution of the direction for different samples in the PAR sections: (▤) INI, (▨) DEF1 and (■) DEF2. When direction = 90° the large axis of the inertia ellipse is parallel to the direction of P. 0 and 180° are equivalent directions.

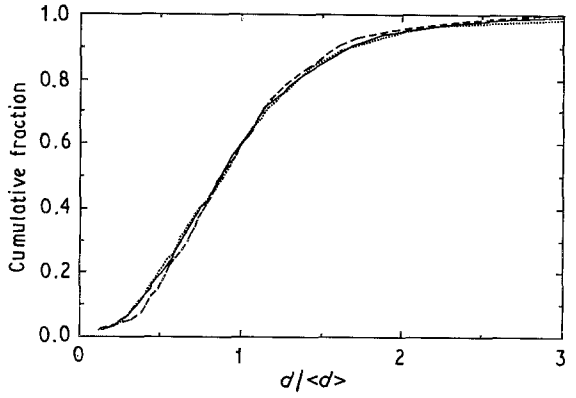

Figure 6 Experimental cumulative distributions of the equivalent normalized diameter ($d/\langle d\rangle$) measured for the different samples. (see Table I for codes): (– – –) INI, (——) AN and (. . . .) DEF2.

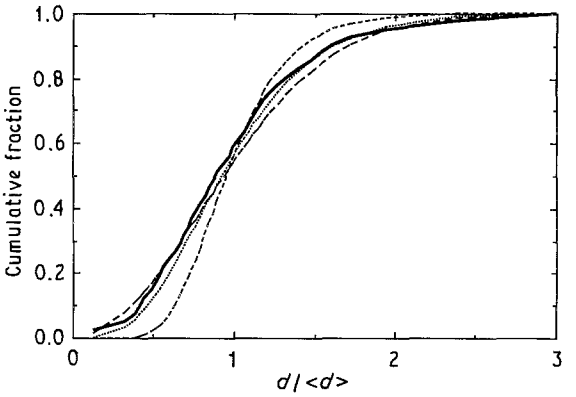

Figure 7 Comparison of theoretical and experimental cumulative distributions of the equivalent normalized diameter: (——) experimental, (. . . .) Γ-function, (- - -) lognormal and (– –) Rayleigh.

deformation is performed during the strain rate plateau regime.

From these results concerning the shape and orientation, it can be concluded that for samples for which GAR ≈ 1 the grains are not equiaxed, the eccentricity being not equal to zero, but their preferential orientation is not sufficiently pronounced to affect GAR. For the samples deformed during the plateau regime the grains are more elongated, and therefore the mean eccentricity increases and their preferential orientation is sufficiently important to affect GAR. In these last samples the value of GAR and the distribution of the directions show that the grains are flattened in the direction of σ.

The cumulative distribution of the normalized equivalent diameter ($d/\langle d\rangle$) is shown in Fig. 6 for different samples; for all of them this distribution was apparently independent of the thermomechanical treatments. Grain growth can then be considered as normal [13] and the distribution of the grain equivalent diameter can be expressed as

$$F(d, t) = G(d/\langle d\rangle)\,\langle d\rangle(t)$$

where $\langle d\rangle(t)$ is the evolution of mean equivalent diameter with time. Such a result shows that the distribution of the normalized diameter was not affected by the grain flattening occurring during creep, which was described in the previous paragraph. Furthermore, no direct relationship between the grain size and shape was observed. These experimental distribution curves were fitted to the most common theoretical ones: lognormal, Rayleigh function and gamma (Γ)-function [14] ; these functions were calculated using the experimental values of the mean grain size and variance. As is shown in Fig. 7, where the different theoretical curves and an experimental one are reported, the best fit was obtained with the Γ-function. Statistical tests (χ^2, Kolmogoroff–Smirnoff) have been applied to evaluate quantitatively the difference or the similarity between these different curves without providing any conclusive result [15]. To our knowledge, no quantitative method has yet been proposed and successfully applied to compare grain size distributions.

Cumulative distribution curves of the eccentricities are shown in Fig. 8 for the different samples. As this parameter is a non-metric one, it would be wrong to use its normalized value. Except for the samples deformed during the plateau, which means at strain levels higher than -0.3 (DEF2 in Fig. 8), this curve is similar for all samples. The shift towards higher values of ecc for the DEF2 sample indicates an elongation of the grains, as does the $\langle$ecc$\rangle$.

The mean values of the different grain shape parameters measured on the two kinds of sections (PAR and PER) of the samples hot-pressed and deformed to -0.5 are shown in Fig. 9; the linear grain sizes reported here are the feret diameters in the corresponding directions. In the hot-pressed state (INI) $\bar{d}$ appears to be slightly larger in the PER section but $\langle$ecc$\rangle$ is the same as in the PAR section.

In the DEF2 sample the grains were significantly larger in the PER section, but the values of ecc and GAR were the same as in the hot-pressed state. In the PAR section, as mentioned above, the grains were flattened in the direction of σ and the feret diameter in the direction of P was larger when P and σ were perpendicular in this section (see Fig. 1). The values of the feret diameters in the PER section were very similar to the larger one in the PAR section. These results obtained with the feret diameter were also

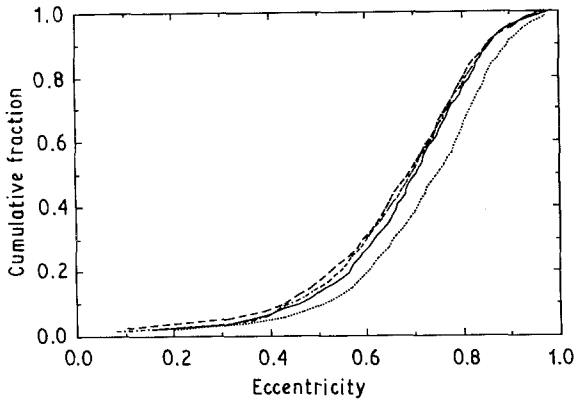

Figure 8 Cumulative distributions of eccentricities for the different samples measured in the PAR sections: (– – –) INI, (— – –) AN, (–·–) DEF1 and (. . . .) DEF2.

obtained when considering $\bar{l}$ as the linear grain size. From these observations it can be concluded that when deformation occurs in the plateau regime, grains become ellipsoidal with two large axes in the plane normal to σ. This shape reflects the stress state due to the applied external stress. If the samples were deformed in uniaxial tension in the plateau regime, grains would become ellipsoids with two short axes in the plane normal to the applied stress, giving an appearance similar to a rugby ball.

In addition, these results show that in the plateau regime the grain shape changes in the same way that the sample does at the macroscopic level. Assuming that grain growth and grain shape modification are two independent processes, the effects of these two phenomena on the linear dimensions of the grain in different directions can be calculated separately. During grain growth the grain shape does not change. The ratio between the linear dimension of the grain before and after grain growth is independent of the direction: for example, $l_x^R = kl_x^I$, where the subscript x refers to the direction and the superscripts R and I refer to initial and annealed samples, respectively. For example, after deformation of an annealed sample by applying an external stress σ in the x-direction, the deformation of the grain in the x-direction is

$$\varepsilon_x = \ln (l_x^D/l_x^R)$$

where the superscript D refers to the deformed state. As the stress state is uniaxial, $\varepsilon_y = \varepsilon_z$. If the volume of the grain does not change during the deformation step, ε_x can be calculated from the mean linear dimensions of the initial and deformed samples assuming that $s \approx l_x l_y$:

$$\varepsilon_x = \ln \left(\frac{(s^I)^{1/3} l_{\|P^D} (l_{\|P^I})^{1/3}}{(s^D)^{1/3} l_{\|P^I} (l_{\|P^D})^{1/3}} \right)$$

Fig. 10 shows the evolution of ε_x with the deformation (ε) of the samples. It can be seen that when deformation occurs during the plateau, the grains have almost the same deformation as the sample ($\partial\varepsilon_g/\partial\varepsilon \approx 1$). As it has been shown that for this composition the plateau is related only to the grain size [10], this plateau can be observed from the beginning of the deformation. In this case the same grain shape change was observed as deformation proceeded during the plateau regime. Such a grain shape evolution suggests that dislocations could be active inside the grains during the plateau regime.

4. Conclusion

A semi-automatic image analysis method was applied to study the evolution of the grain shape and size during high-temperature compressive creep of yttria-doped alumina. It was shown that grains flatten in the direction of σ when deformation occurs during the strain rate plateau that is characteristic of this material. This flattening of the grains did not affect the normalized grain size distribution function. This function can be best approximated by a Γ-function. Characterization of differently oriented sections showed that the grains followed the same shape change as the sample at the macroscopic level when

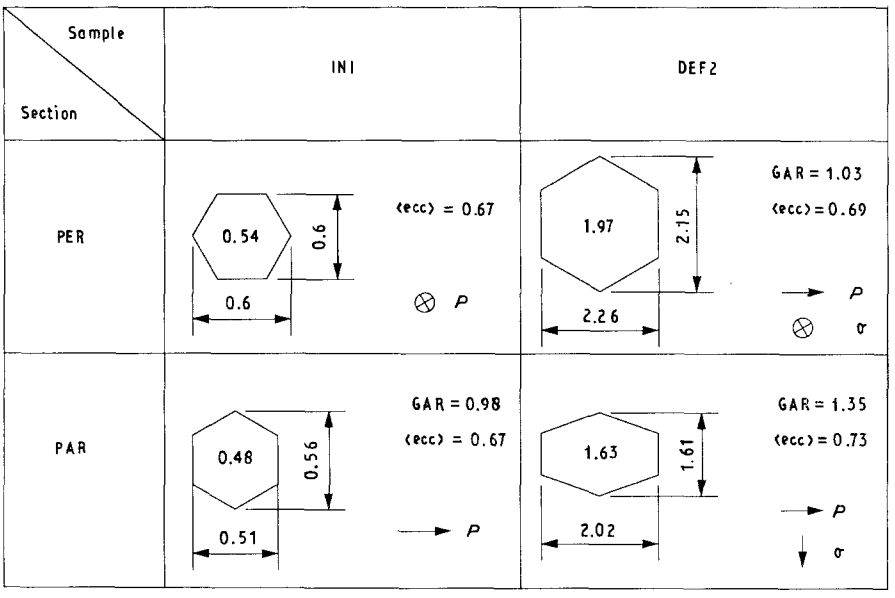

Figure 9 Schematic representation of mean values of the parameters measured on the PER and PAR sections for the samples INI and DEF2.

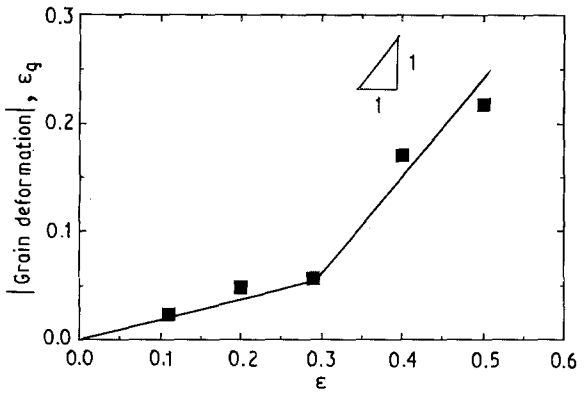

Figure 10 Evolution of the absolute value of the calculated deformation of the grain (ε_g) with the absolute deformation of the sample (ε).

deformation proceeded during the plateau regime; in this case the calculated strain of the grains was similar to that of the sample.

Acknowledgements

This work was partially supported by the Swiss National Foundation and by the Swiss Federal Office for Education and Science as a part of the COST 503 European programme. The programming of the statistical tests was performed by Mr. H. Boel.

References

1. F. RIGHETTI, H. TELLEY, T. LIEBLING and A. MOCELLIN, *Comput. Phys. Commun.* **67** (1992) 509.
2. M. A. CLARK and T. H. ALDEN, *Acta Metall.* **21** (1973) 1195.
3. D. S. WILKINSON and C. H. CACERES, *ibid.* **32** (1984) 1335.
4. J. D. FRIDEZ, C. CARRY and A. MOCELLIN, in "Advances in Ceramics", Vol. 10, edited by W. D. Kingery (American Ceramic Society, Westerville, Ohio, 1985) p. 720.
5. J. D. FRIDEZ, Thesis, EPFL, Lausanne (1986).
6. K. R. VENKATACHARI and R. RAJ, *J. Amer. Ceram. Soc.* **69** (1986) 135.
7. L. A. XUE and I. W. CHEN, *ibid.* **73** (1990) 3518.
8. B. BURTON, in "Diffusional Creep of Polycrystalline Materials". Diffusion and Defects Monograph Series (Trans. Tech. Publ., 1977).
9. B. P. KASHYAP and A. K. MUKHERJEE, in "Superplasticity", edited by B. Baudelet and M. Suéry (Centre National de Recherche Scientifique, Paris, 1985) p. 4.1.
10. P. GRUFFEL and C. CARRY, in Proceedings of the 11th International Symposium on Metallurgy and Materials Science, Risø, September 1990, edited by J. J. Bentzen, J. B. Bilde-Sørensen, N. Christiansen, A. Horsewell and B. Ralph (Roskilde, Denmark, 1990) p. 305.
11. P. GRUFFEL, Thesis, EPFL, Lausanne (1991).
12. E. E. UNDERWOOD, in "Quantitative Stereology" (Addison-Wesley, 1970).
13. A. MOCELLIN, in Proceedings of NATO–ASI, 1989, edited by L. C. Dufour C. Monty and G. Petot-Ervas (Kluwer Academic, 1989) p. 485.
14. M. F. VAZ and M. A. FORTES, *Scripta Metall.* **22** (1988) 35.
15. H. BOEL, Internal Report LCE/DMX/EPFL, Lausanne, (1988).

Received 13 September 1991
and accepted 2 September 1992